JACS
JOURNAL OF THE AMERICAN CHEMICAL SOCIETY

ARTICLE

pubs.acs.org/JACS

Encapsulation of Metal Cations by the PhePhe Ligand: A Cation−π Ion Cage

Robert C. Dunbar,*[,†] Jeffrey D. Steill,[‡,§] and Jos Oomens*[,‡,∥]

[†]Chemistry Department, Case Western Reserve University, Cleveland, Ohio 44106, United States

[‡]FOM-Institute for Plasma Physics Rijnhuizen, Edisonbaan 14, NL-3439 MN Nieuwegein, The Netherlands

[∥]University of Amsterdam, Science Park 904, 1098 XH Amsterdam, The Netherlands

Supporting Information

ABSTRACT: Structures and binding thermochemistry are investigated for protonated PhePhe and for complexes of PhePhe with the alkaline-earth ions Ba^{2+} and Ca^{2+}, the alkali-metal ions Li^+, Na^+, K^+, and Cs^+, and the transition-metal ion Ag^+. The two neighboring aromatic side chains open the possibility of a novel encapsulation motif of the metal ion in a double cation−π configuration, which is found to be realized for the alkaline-earth complexes and, in a variant form, for the Ag^+ complex. Experimentally, complexes are formed by electrospray ionization, trapped in an FT-ICR mass spectrometer, and characterized by infrared multiple photon dissociation (IRMPD) spectroscopy using the free electron laser FELIX. Interpretation is assisted by thermochemical and IR spectral calculations using density functional theory (DFT). The IRMPD spectrum of protonated PhePhe is reproduced with good fidelity by the calculated spectrum of the most stable conformation, although the additional presence of the secondmost stable conformation is not excluded. All metal-ion complexes have charge-solvated binding modes, with zwitterion (salt bridge) forms being much less stable. The amide oxygen always coordinates to the metal ion, as well as at least one phenyl ring (cation−π interaction). At least one additional chelation site is always occupied, which may be either the amino nitrogen or the carboxy carbonyl oxygen. The alkaline-earth complexes prefer a highly compact caged structure with both phenyl rings providing cation−π stabilization in a "sandwich" configuration (OORR chelation). The alkali-metal complexes prefer open-cage structures with only one cation−π interaction, except perhaps Cs^+. The Ag^+ complex shows a unique preference for the closed-cage amino-bound NORR structure. Ligand-driven perturbations of normal-mode frequencies are generally found to correlate linearly with metal-ion binding energy.

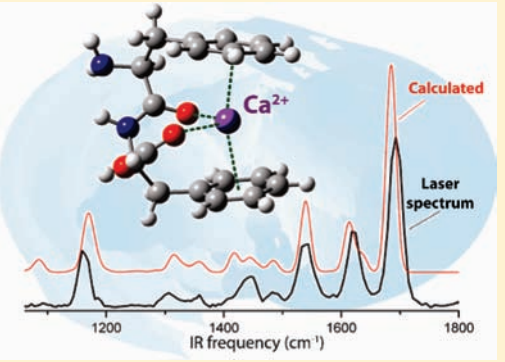

1. INTRODUCTION

Sandwiching of metal ions between planar aromatic structures is a frequent motif in organometallic chemistry. Innumerable sandwich complexes following the ferrocene architecture or the dibenzene/metal architecture are known, for example. A comparable but more extended architecture is shown for instance by graphite intercalation complexes such as calcium graphite $(CaC_6)_x$ having metal ions sandwiched between infinite aromatic carbon sheets.[1] In the gas phase, many dibenzene complexes of metal ions are known (including many with substituents). The structures of these "dimeric" metal-ion complexes are frequently assigned as sandwiches on the basis of quantum-chemical calculations, while the emergence of spectroscopic techniques applicable to gas-phase ionic and neutral complexes has furnished experimental support for such structure assignments in a small but growing number of cases.[2−6] The possible astrochemical importance of metal-ion sandwiches with planar aromatic molecules, in particular polycyclic aromatic hydrocarbons (PAH's), has also been a steady theme of this organometallic chemistry over many years.[7,8]

For Ca^{2+}, Figure 1 sets the chemical context of the cation−π cage suggested in the present study. Illustrated are the calcium−graphite intercalation compound,[1] the calcium ion−benzene sandwich complex, and the PhePhe caged structure suggested here. The (measured) inter-ring distance for calcium−graphite is the shortest, while the (calculated) distances for $Ca(benzene)_2^{2+}$ and $Ca(PhePhe)^{2+}$ are somewhat larger.

Cation−π interactions are increasingly considered as playing structure-forming as well as functional roles in metal-ion complexation in biological systems, and we can give a few examples from the extensive literature concerning the appearance of this motif in actual biological systems[9−13] and the structural and thermodynamic aspects of such interactions in model systems.[5,6,10−12,14−23]

It is intriguing to consider the possibly enhanced role of a doubled cation−π interaction with sandwiching of the metal between two aromatic rings in both biological systems and other

Received: January 20, 2011
Published: May 09, 2011

dx.doi.org/10.1021/ja200219q | J. Am. Chem. Soc. 2011, 133, 9376–9386

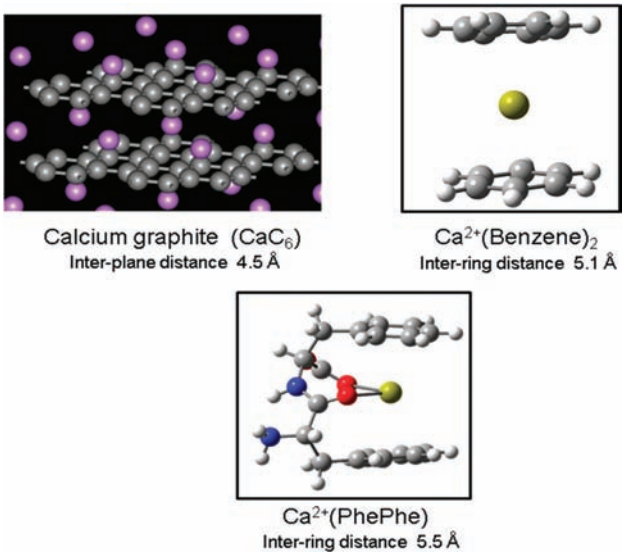

Figure 1. Sandwiching motifs for metal ions between π-electron sheets (inter-ring distance and image of calcium graphite from Wikipedia (materialscientist; http://en.wikipedia.org/wiki/File:CaC6structure.jpg); distances for the complexes calculated using the computational protocol of the present study).

organometallic complexes. For instance, Gokel's group has shown the favorability of encapsulation of metal ions by sandwiching aromatic side chains in the lariat ether systems and has considered the cation$-\pi$ binding of alkali-metal ions to aromatic amino acid models in numerous publications.[18,24,25] In the gas phase, the study of the thermodynamics and structures of metal-ion complexes with aromatic amino acids,[21,26−35] small peptides,[23,36−45] and even proteins[46] has been addressed by many groups. The present encapsulation motif furthermore relates to the binding of metal ions in calixarene systems, where cation$-\pi$ interactions with multiple aromatic rings are also found.[47]

More speculative is the possible connection between cation$-\pi$ interactions and the functioning of metal cation channels in biological membranes. An accumulation of aromatic residues has been taken to suggest roles for cation$-\pi$ interactions in the functioning of ion channels (for example, refs 13,15, and 48). A suggestive specific observation in line with this generalization is the conserved appearance of a pair of adjacent aromatic residues (FF, FY, YF, or YY) at the position 4 past the extracellular terminus of the 25-residue transmembrane-spanning segment S-6, which appears in 4 repeats in the pore-forming α-1 subunit of the family of voltage-regulated Ca^{2+} channels.[49] Within this broad family of channel proteins this double-aromatic element shows up strongly conserved in mammals and fish, conserved with slight variations for fruit flies and bees, and recurs with wider variations in invertebrates and plants.[50] As another speculative possibility for the manifestation of multiple cation$-\pi$ binding involving ion channels, we mention a set of compounds having two pendant Lewis basic groups that recently generated a patent application for their ability to block calcium membrane-transport channels. The compounds ranking highest in a complexation-assay comparison of this series of molecules were those having aromatic pendant groups.[51]

Crystal structures are known for sandwiched Ru(II) complexes in which one face of the sandwich is supplied by Phe or cyclo-PhePhe, while the other face is supplied by cymene (4-methylisopropylbenzene).[52] In another analogy, the structure assigned to the 2:1 complex of the drug verapamil to Ca^{2+} positions the calcium ion in a cation$-\pi$ interacting geometry to two of the four available aromatic rings.[53]

Although the examples noted here suggest possibilities of double cation$-\pi$ interactions in various biological or model biological systems, we have not found a known precedent for the sandwiching encapsulation motif with PhePhe or similar double-aromatic residue pairs as suggested here. No role for double-aromatic metal-ion binding has actually been demonstrated, but the present report of the excellent stability of this motif, particularly for the divalent calcium ion, could open new possible lines of thought. Forming a background for the present study, the binding of alkalis metals to phenylalanine in particular has been studied at a high level of computational theory.[29]

Motivated by thinking about possible roles of double cation$-\pi$ sandwich binding, and following on various previous studies by our research groups of gas-phase cation$-\pi$ binding involving aromatic amino acids[4,31−33,54−56] and dipeptides,[37,40] as well as nonbiological aromatic ligands,[57,58] we explore here the binding of metal ions by the doubly aromatic dipeptide ligand PhePhe (phenylalanyl phenylalanine). While sandwich-type complexes have been studied spectroscopically for systems of mainly catalytic interest,[6] biological ligands with multiple aromatic moieties have not been characterized with gas-phase spectroscopy thus far. We present gas-phase infrared spectra of the metal-ion ligand complexes in combination with theoretical investigations, which provide detailed insights into the competition between the double cation$-\pi$ "sandwich" structure as compared to other binding motifs and how these preferences are influenced by cation size and charge. As the present study shows, a double cation$-\pi$ binding motif offers an attractive, high-symmetry possibility for encapsulation of the metal ion, but the energetic and entropic penalties incurred in this compact folding are sufficient to make other alternatives possible. The recent development of gas-phase spectroscopic tools for ion structure analysis,[4,59] and reliable computational tools for comparing structure-dependent thermochemistry, make it possible to address this challenging ion-structure problem.

2. EXPERIMENTAL AND COMPUTATIONAL DETAILS

2.1. Computation. Calculations were performed using Gaussian03,[60] at the B3LYP/6-311+g(d,p) level unless otherwise noted, fully geometry optimized. No imaginary frequencies were encountered. For economy, some of the structures found to lie far above the ground-state energy were calculated at the faster double-ζ level, B3LYP/6-31+g(d,p), and this level was used for some of the computed spectra. For Rb^+, Cs^+, Ba^{2+}, and Ag^+ the sdd relativistic effective core potential was used. Energies were corrected for zero-point energy effects and for thermal energy at 298 K. The computed frequencies were scaled by 0.975 (6-31+g(d,p) or 0.98 (6-311+g(d,p)), as has been found appropriate in previous analyses of IRMPD spectra of cationized amino acids and small peptides in this wavelength range.[31,32,54] They were convoluted with a Gaussian line shape with a fwhm of 30 cm^{-1} for visual comparison to experimental spectra. Free energy values were based on an assumption of rigid-rotor/harmonic-oscillator contributions to the entropies. The aim of this study was not to obtain accurate binding thermochemistry of these systems; therefore, no basis set superposition corrections were applied except as noted.

Recently it has been suggested that the Def2TZVP basis[61] gives better thermochemical results than 6-311+g(d,p) for large metal-ion complexes.[62,63] This was tried for a few cases, some of which are noted

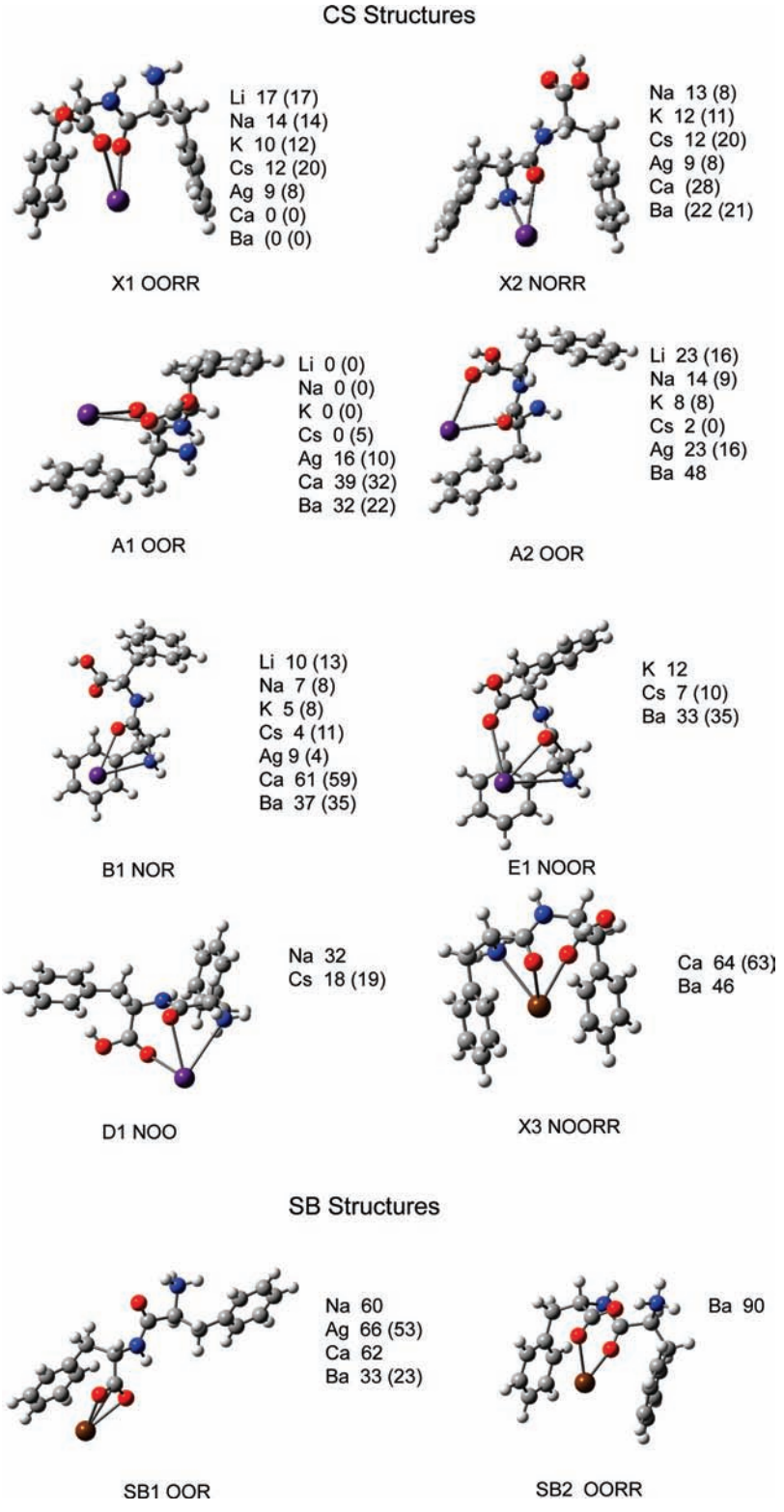

Figure 2. Low-energy conformational patterns of the metal-ion/PhePhe complexes. Energies (as also shown in Table 1) are relative to the lowest conformation that was located for each metal ion. Free energies (in kJ/mol in parentheses) are relative to the conformation of lowest free energy. Cs^+ complexes are shown for illustration (except X3, SB1, and SB2, for which the Ba^{2+} complex is shown).

below, but no major, crucial energy differences from the 6-311+g(d,p) results were uncovered, while the computed spectra were found in all cases to be very similar. The somewhat unexpected energetic preference found for the charge-solvated conformation of Ba^{2+}PhePhe over the zwitterionic conformation motivated confirmatory calculations at the levels of B3LYP/Def2TZVP and MP2(full)/6-311+g(d,p), which did not give significantly different results. It is well-known that B3LYP is not the best functional for treating dispersion interactions, and future

dx.doi.org/10.1021/ja200219q |*J. Am. Chem. Soc.* 2011, 133, 9376–9386

Table 1. Computed Conformational Energies Relative to the Most Stable Conformation (in kJ/mol)[a]

	Li^+	Na^+	K^+	Cs^+	Ag^+	Ca^{2+}	Ba^{2+}
X1 (OORR)	17 (17)	14 (14)	10 (12)	12 (20)	9 (8)[c]	0 (0)	0 (0)
X2 (NORR)		13 (8)[b]	12 (11)	10 (12)	0 (0)[c]	28	22 (21)
A1 (OOR)	0 (0)	0 (0)	0 (0)	0 (5)	16 (10)[c]	39 (32)	32 (22)
A2 (OOR)	23 (16)	14 (9)	8 (8)	2 (0)	23 (16)		48
B1 (NOR)	10 (13)	7 (8)	5 (8)	4 (11)	9 (4)[c]	61 (59)	37 (35)
B1′ (NOR)	13 (10)	9 (6)	7 (6)	6 (10)	9[c]	64	39
E1 (NOOR)		[d]	12	7 (10)	[d]	54	33 (35)
X3 (NOORR)						64 (63)	46
D1 (OON)		32		18 (19)			
SB1 (OOR)		60			66 (53)	62	33 (23)
SB2 (OORR)							90
O—M^+ bond (Å)	1.88	2.21	2.57	2.93	2.56	2.27	2.50

[a] Free energies (given in parentheses) are relative to the conformation with lowest free energy. The metal-ion/amide oxygen distances (Å) are listed for the most stable conformation of each complex as a relative measure of the sizes of the metal ions. [b] Structure opens. [c] MPW1PW91. [d] Structure opens to B1′.

workers on metal-ion−π interacting systems will want to test functionals now becoming recognized to perform better in this regard.[64] However, we believe that this deficiency of B3LYP may not be relevant to the interactions of concern in systems like the ones studied here. These are dominated by the ion/neutral polarization energy and the ion/multipole Coulomb energy, which is different in character and much stronger than the neutral/neutral dispersion interactions of concern in neutral systems such as van der Waals complexes. There does not seem to be compelling evidence that B3LYP or its cousins fail seriously to reflect the ion/neutral polarization and Coulomb energies.

2.2. Experiment. Infrared spectra of the ionized gas-phase complexes were measured using an action-spectroscopic approach based on a combination of IR laser spectroscopy and fourier transform ion cyclotron resonance (FTICR) mass spectrometry,[3,4,65] in particular IR multiple photon dissociation (IRMPD) spectroscopy. The FTICR mass spectrometer interfaced to the FELIX free-electron laser light source at the FOM Institute (Rijnhuizen) was used, as has been described in detail.[66,67] Ions were produced by electrospray ionization (ESI) from a methanol/water solution of the peptide and the metal salt (metal chloride or nitrate), usually at a 1 mM concentration of each. Ions were accumulated and stored for collisional and radiative cooling during 4 s in a hexapole linear trap, followed by mass isolation in the FTICR ion trap and irradiation by FELIX for typically 3 s. The IR spectrum was reconstructed by summing all major fragment ions and plotting the total fragment yield as a function of the photon energy.

A linear correction corresponding to the measured laser intensity as a function of wavelength was applied, and the laser wavelength was calibrated two or three times a day, or after a change in laser parameters. A linear power dependence correction has been consistently applied in many IRMPD spectroscopy studies and is believed to give a frequently appropriate approximate correction over the moderate variations of laser power encountered in the present work (up to a factor of 2 at the extreme edges of the spectral tuning range).

3. RESULTS

3.1. Structural Motifs and Thermochemistry. *3.1.1. Cationized Complexes.* Figure 2 displays the structural themes surveyed in the calculations. In the previous survey of alkali-metal-ion PheAla and AlaPhe complexes,[37] two relevant features emerged regarding the favorable chelation patterns in phenylalanine-related dipeptides. First, the amide carbonyl group is always coordinated to the metal ion, and two additional chelation points are normal, which can be chosen from three possibilities: the terminal nitrogen, the COOH carbonyl, and the aromatic ring. Binding energies for these last three options are fairly similar. However, chelates including the phenyl ring were somewhat better than those with the ring uncoordinated. Tetradentate chelation was possible but was not as favorable as the best tridentate conformations. Second, chelation involving the aromatic ring is favorable when Phe is the N-terminal residue but more difficult when Phe is the C-terminal residue. For example, in the case of Ba^{2+}AlaPhe, the complex prefers to adopt a zwitterion conformation (no cation−π coordination to the C-terminal side chain ring), whereas the corresponding complex with PheAla prefers a charge-solvated conformation involving cation−π coordination to the aromatic ring of the N-terminal side chain.[40]

These characteristics are echoed in the PhePhe complex structures shown in Figure 2. The thermochemical consequences are shown in Table 1. No bidentate conformations were found to be energetically competitive with more highly chelated structures. Some tetradentate and pentadentate structures were reasonable, but all of the ground states are tridentate. Among the open conformations (that is, those which do not enclose the metal ion between two rings), the aromatic ring of the N-terminal Phe residue is always the ring that is bound. The D1 conformation, having no ring chelation, is not energetically hopeless for Cs^+, at least, but is significantly less stable than numerous ring-chelated possibilities, underscoring in general the importance of cation−π interactions. Intramolecular interactions in the vicinity of the metal ion dominate the thermochemical variations: This is illustrated by the B1 and B1′ structures, which differ only in the orientation of the remote side chain and which show insignificant differences in their thermochemistry and IR spectra.

The most interesting and important new feature of PhePhe in comparison with PheAla and AlaPhe is the emergence of the caged (closed) structures such as X1, X2, and X3, which of course were not a possibility for the PheAla and AlaPhe ligands. Notably, for the alkaline-earth-metal ions (barium and calcium) this is far and away the best structural type, reflecting the fact that the doubly charged metal ion is so strongly solvated by cation−π interactions that it easily overcomes any steric-strain and

dx.doi.org/10.1021/ja200219q | J. Am. Chem. Soc. 2011, 133, 9376–9386

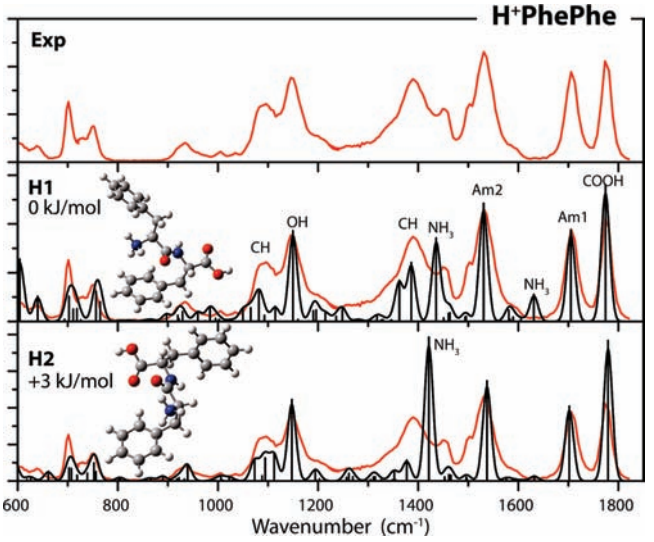

Figure 3. Experimental spectrum of H^+PhePhe (top panel) and calculated spectra of the two low-energy conformations (lower panels) using the triple-ζ (B3LYP/6-311+G(d,p)) basis set. Band labels indicate the main vibrational character, where Am1 and Am2 refer to amide I (amide C═O stretch) and amide II (amide NH bend), respectively.

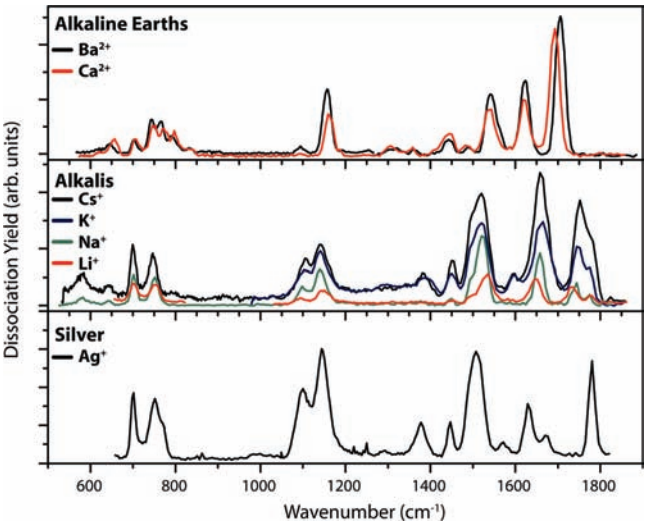

Figure 4. Experimental IRMPD spectra of cationized PhePhe complexes.

entropic disadvantages in order to achieve solvation by both phenyl rings. The case is reversed for the alkali metals, where the singly charged metal ion does not interact as strongly with the rings and is unable to force the C-terminal ring into chelation. Thus, the open structures (the A1 (OOR) and B1 (NOR) families) are preferred over the caged structures for all alkali metals.

3.1.2. Protonated PhePhe. For amino acids and dipeptides not having exceptionally basic side-chain sites, the terminal nitrogen is the most basic site toward protons. The two families of N-terminal protonated conformers H1 and H2, differing in energy by only 3 kJ/mol, were located, as shown in Figure 3. These correspond respectively to the conformer family I (anti) and family I (gauche) found by Stearns et al. to be lowest in energy for protonated TyrAla.[41]

3.2. Spectra and Conformations. *3.2.1. Protonated PhePhe.* The infrared spectroscopy of these complexes can solidify many of the structural conclusions derived from the calculated thermochemistry described above. In the case of the protonated peptide, Figure 3 displays the IRMPD spectrum and the calculated spectra of the two low-energy conformers. Double-ζ and triple-ζ computations gave virtually identical spectra, except that the NH_3 umbrella bending mode near 1400 cm^{-1} is shifted by 5−10 cm^{-1} to the blue region with the higher level basis. All of the predicted modes of the most stable H1 conformation having significant intensity, with the exception of the weak NH_3 mode near 1620 cm^{-1}, show thoroughly convincing matches between the experimental and calculated spectra. The match to the second-most stable conformation, H2, is practically as good, apart from the intense NH_3 mode calculated to lie just above 1400 cm^{-1}. A fraction of the population having the latter structure is certainly not ruled out on the basis of either the spectroscopy or the calculated relative energies.

The two most stable conformations, H1 and H2, differ in the details of the folding of the peptide chain, but they have in common several key stabilizing characteristics: namely, the protonation at the most basic site (the NH_2 group of the neutral dipeptide), the internal hydrogen bond between the ammonium group and the amide carbonyl oxygen, and the location of the positive charge of the ammonium group in the region of negative potential above the plane of one of the aromatic rings. In the case of H1, the closest ammonium−π interaction involves the ring on the C-terminal side chain, whereas for H2, it involves the side chain on the N-terminal side. However, in the H1 case, there appears to be a second, weaker electrostatic stabilization between the ammonium group's positive charge and the other aromatic ring, so that this complex achieves a very rough semblance of a sandwich geometry. No such interaction occurs in H2, which probably explains the slightly higher stability calculated for H1.

As indicated by the peak labels in Figure 3, we may identify a number of expected vibrational modes in the spectrum. The most obvious of these include the C═O stretch (1780 cm^{-1}) of the carboxyl, the amide I (1700 cm^{-1}) and amide II (1530 cm^{-1}) modes, the umbrella symmetric N−H bend of the ammonium group (1420 cm^{-1}), and the hydroxyl bend (1150 cm^{-1}). The H2 spectrum is very similar to the H1 spectrum, and it is not possible with any confidence to say what proportion of the ion population might be one or the other of these conformers. If the calculated 3 kJ mol^{-1} stability advantage of H1 is accurate, thermal equilibrium would predict an approximately 3:1 ratio of H1 to H2. The somewhat better match of the experimental spectrum with the H1 calculated spectrum in the 1350−1450 cm^{-1} range might also reflect a preponderance of H1.

3.2.2. The Cationized Complexes. 3.2.2.1. Spectroscopic Conformation Assignments. Figure 4 displays the IRMPD spectra of the alkaline-earth-metal complexes, the alkali-metal complexes, and the silver cation complex. The cationized complexes have a great many conformation possibilities, which will be addressed with the help of Figures 5−8 showing experimental and calculated spectra of representative complexes. Spectra for the remaining complexes are given in the Supporting Information, namely calcium (similar in all important respects to barium), sodium (fairly similar to potassium), and silver.

Several conformation issues can be addressed. We can summarize three principal conclusions as follows, with detailed discussions to be given in the following three subsections. (1) All of the complexes have a charge-solvated (CS) mode of

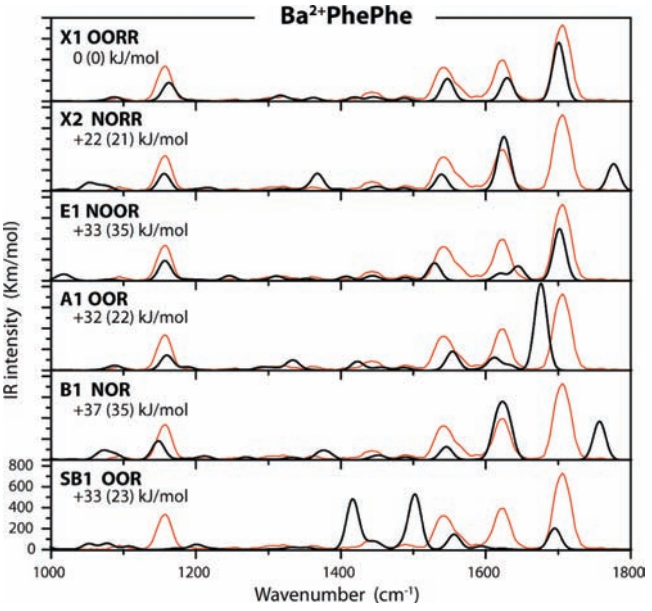

Figure 5. Calculated spectra (black) of various possible Ba^{2+}PhePhe complexes. The IRMPD experimental spectrum is overlaid in red. Energy values are 0 K enthalpies, with room-temperature free energies given in parentheses (kJ/mol).

complexation, with no observable presence of zwitterionic (salt bridge, SB) components in the ion populations. (2) The alkaline-earth-metal complexes and perhaps the Ag^+ complex encapsulate the metal ion in a closed cage involving double cation−π binding of the aromatic rings, while the alkali-metal complexes open the cage so that only one ring chelates the metal ion. (3) Chelation of the metal ion by the amide carbonyl oxygen and cation−π chelation by one or both rings provide two (or three) chelation sites in all cases, and an additional chelation site is provided by choosing either the amino nitrogen or the carboxy carbonyl oxygen. The evidence to be surveyed consists of the calculated thermochemistry of the possible conformations in Table 1 (with the assumption that conformations of high relative stability are likely to dominate the ion population as it is sampled in the ICR ion trap) and the comparison of observed IRMPD spectra with calculated spectra for the possible conformations.

3.2.2.2. Possible Presence of Zwitterions. A competition often exists between the CS and the SB conformations of the cationized peptides. The thermochemical trade-off between these two binding modes is closely balanced for many cases of metal ion binding to mono(amino acid) ligands.[31,62,63,68−80] One of the primary factors pushing the competition in the CS direction is favorable microsolvation of the cationic center, which in turn is favored by the availability of strongly binding Lewis basic side chain groups in strain-free solvating geometries. The PhePhe ligand provides at least one if not two solvating aromatic side chains in a favorable position for cation−π chelation; thus, it is not surprising that the spectra as well as the calculations show a strong preference for CS binding in all of the PhePhe complexes. As suggested by the calculated thermochemistry (Table 1), no case was found where an SB conformation was thermally accessible in competition with CS conformers. The open-geometry SB1 complex of Ba^{2+} was the most favorable one found, having a calculated free energy within 23 kJ/mol of the best CS conformer. An SB closed-cage structure (SB2) was found for barium, but with high energy (+90 kJ/mol). For sodium, no stable SB cage (SB2) was found, since this conformation spontaneously transferred the proton from the NH_3^+ group to the amide oxygen, and similar behavior for the other singly charged ions presumably rules out a closed-cage SB structure in all cases. Even for Ba^{2+}, which has shown the greatest propensity for forming SB complexes among the alkali-metal and alkaline-earth-metal ions, the excellent cation solvation in the closed-cage CS structure X1 far outweighs the factors favoring SB formation for barium complexes, so that SB formation is never thermochemically favorable for any of the metal ions considered here.

To solidify this conclusion, the two representative SB structures shown in Figure 2 can be compared with experiment. The presence of SB complexes would be most strongly signaled by an intense peak near 1400 cm^{-1} corresponding to the NH_3^+ group, as illustrated in the calculated SB1 spectrum of Ba^{2+}PhePhe (SB1) shown in Figure 5. No significant intensity is seen in any of the IRMPD spectra near this position, ruling out a significant contribution of SB1 complexes in the populations.

3.2.2.3. Choice of Chelation by the Amino Nitrogen versus the Carboxy Carbonyl Oxygen. The division of the complexes into those having metal chelation by the amino nitrogen versus those having chelation by the carboxyl carbonyl oxygen is a useful principle, because these two chelation sites do not appear to be occupied simultaneously in any case, and the spectroscopic diagnostic of which one is occupied (via the position of the carboxyl C═O stretch mode) is highly distinctive.

The spectra of all four alkali-metal complexes show a splitting of the carboxyl C═O stretch (1740−1770 cm^{-1}), which reflects the simultaneous presence of two different environments for the carboxyl group. This splitting is attributed to mixed populations of complexes, with the low-frequency component having the carboxyl carbonyl oxygen chelated to the metal ion and the high-frequency component having this oxygen unbound and the metal chelated by the amino nitrogen instead. Each of the alkali-metal spectra accordingly requires the assignment of two structures, taken to be A1 and either B1 or B1′. The alkaline-earth metals and the silver ion do not show evidence of a mixture of these two binding motifs (see Figure 4) but do show an interesting contrast between the silver complex, which prefers amino binding (X2 NORR or B1 NOR), versus the alkaline-earth-metal complexes, which prefer carboxyl binding (X1 OORR) (see Table 1, Figure 5, and Figures S1 and S2 (Supporting Information)).

3.2.2.4. Conformation Assignments and the Characterization of Open versus Closed Cage. For some of the carboxy-chelated complexes, it was found that at least one open-cage and at least one closed-cage conformation gave calculated spectra that could reasonably be matched to the observed spectrum. This was also true for the amino-chelated complexes of K^+ and Cs^+. Thus, the mid-IR spectroscopic evidence is not always a definitive route to distinguishing open versus closed character, and often it was necessary to combine spectroscopic evidence with arguments from thermochemical stability in order to make an assignment. Ion mobility measurements[81] may form an alternative tool for distinguishing these conformations, since the open structures likely have larger cross sections than the closed structures, and such studies are planned for the future.

The alkaline-earth-metal spectra have a clean appearance, having a small number of prominent features, no indication of clutter, congestion, or overlapping peaks from conformer mixtures, and reasonably narrow bands in terms of typical room-temperature IRMPD spectra of large-molecule complexes.

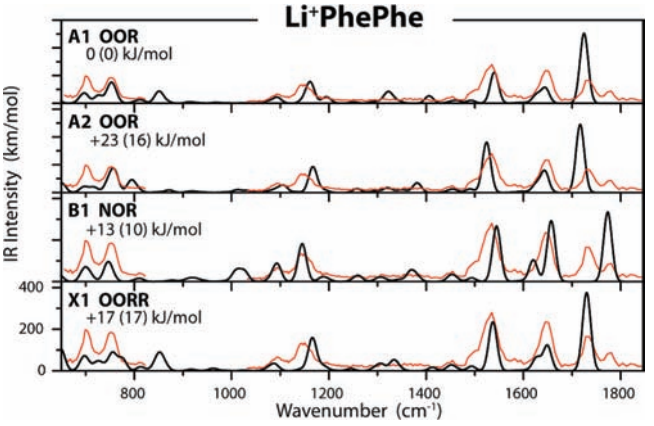

Figure 6. Calculated spectra (black) of various low-energy conformers of Li^+PhePhe. The IRMPD experimental spectrum is overlaid in red. Energy values are 0 K enthalpies, with free energies given in parentheses (kJ/mol).

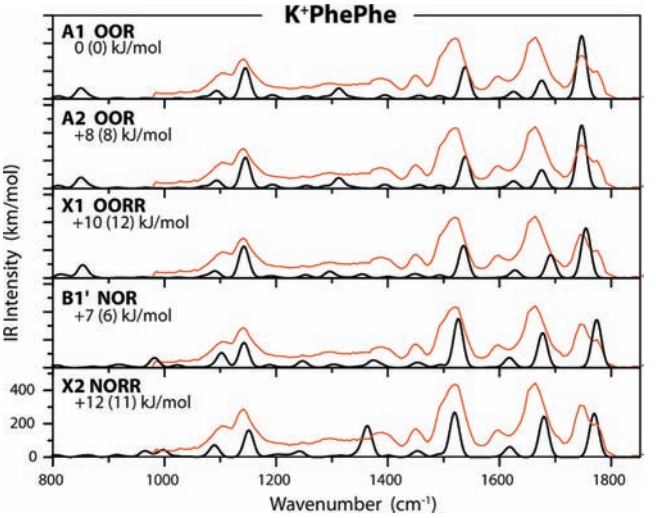

Figure 7. Calculated spectra (black) of several low-energy K^+PhePhe complex structures. The IRMPD experimental spectrum is overlaid in red. Energy values are 0 K enthalpies, with free energies given in parentheses (kJ/mol).

All signs are that these spectra reflect a single conformer. Figure 5, showing the complex with Ba^{2+}, suggests that the closed-cage structure X1 OORR provides an excellent match to the observed spectrum. The open-cage variant E1 NOOR is the only other conformer that could contribute on spectroscopic grounds, but it is unreasonable in view of its poor stability (+33 kJ mol^{-1}). Other open-cage variants such as A1 or B1 are unacceptable on both thermochemical and spectroscopic grounds. (The best of these thermochemically is A1, which is 22 kJ mol^{-1} above the ground state but has a very poorly matching spectrum.) The situation with Ca^{2+} is similar (Figure S2 (Supporting Information)): the calculated spectrum of the closed-cage X1 (OORR) conformation gives an excellent spectroscopic match, and X1 is by far the most stable of the conformations surveyed. We conclude that the alkaline-earth-metal complexes definitely have the closed-cage geometry with double cation$-\pi$ binding and OORR chelation. The metal is equidistant from both rings and is centered over each ring with good accuracy (η^6 to both rings). The metal-to-ring-plane distance is 2.7 Å for Ca^{2+} and 3.1 Å for Ba^{2+}. The rings show little distortion; for Ca^{2+}, the C$-$C distance in the coordinated rings grows slightly to an average 1.408 Å from an average of 1.399 Å for uncoordinated rings at the same computational level.

With the alkali-metal ions the situation is quite different. The spectra show much more complexity and larger line widths, suggesting partially unresolved bands and probable conformational mixing or flexibility. Consider first the assignment of the carboxy-coordinated conformations. For Li^+, the closed-cage simulated spectrum (X1 OORR) gives just as good a match to the experimental spectrum as the open-cage structures (Figure 6). For Na^+ and K^+ complexes, the simulated closed-cage X1 OORR spectrum does not match quite as well as the open-cage A1 OOR spectrum, but the difference is relatively small and arguably not definitive (see Figure 7 and Figure S3 (Supporting Information)). However, for all three of the Li^+, Na^+, and K^+ complexes, the closed-cage structure has significantly higher free energies than the open-cage A1 OOR structures (higher by 12$-$20 kJ/mol), and we assign open-cage structures to these three complexes with reasonable confidence. For Li^+ and Na^+, the characterization of the X1 conformation as "closed" is actually imprecise, because the second ring does not move into a true cation$-\pi$ binding position but is instead relatively remote from the metal ion and is also strongly displaced laterally from a symmetrical position over the metal. This failure to form structures with true double cation$-\pi$ sandwiches is reflected in the calculated spectra for these two cases, in that the calculated spectra of the nominal X1 closed-cage conformations are essentially identical with those of the "open" A1 or A2 structures. The K^+ complex appears more willing to form a proper closed-cage sandwich-type complex, although, as already noted, it has poorer stability than the open-cage alternatives and is not considered likely to be a significant contributor to the population.

Only for Cs^+ is the match of the calculated closed-cage X1 OORR spectrum sufficiently poor that we can give a convincing spectroscopic argument against the closed cage for the carboxyl-bound species. This gives spectroscopic confirmation of the argument on the basis of the better calculated stability of the open-cage structures. In the Cs^+ case, as distinct from the smaller alkali metals, an OOR chelation pattern is still assigned, but with a variant conformation. Here, the A2 OOR conformation is calculated to be more stable than A1 OOR, as well as giving a better spectroscopic match, and we assign an open-cage geometry with the A2 structure to the carboxyl-bound component of the Cs^+ complex. Thus, in summary we assign an open-cage character as the predominant carboxyl-bound conformations for all the alkali-metal complexes, with a switch from A1 to A2 for the largest metal ion (Cs^+).

Considering the amino-bound alkali-metal complexes identified by the peak or shoulder near 1780 cm^{-1}, the smaller and larger alkali-metal ions must be distinguished. For Li^+ and Na^+, attempted calculations of a closed-cage NORR conformation gave no potential energy minimum, having the second ring in a cation$-\pi$ bound position. The B1 NOR conformation is a very satisfactory match to the observed spectra and is the only amino-bound conformation of reasonable stability found in the calculations. Accordingly we assign this open-cage structure to the Li^+ and Na^+ complexes (but we note that for Na^+, at least, it does not cost much energy to move the second ring into a cation$-\pi$

dx.doi.org/10.1021/ja200219q | J. Am. Chem. Soc. 2011, 133, 9376–9386

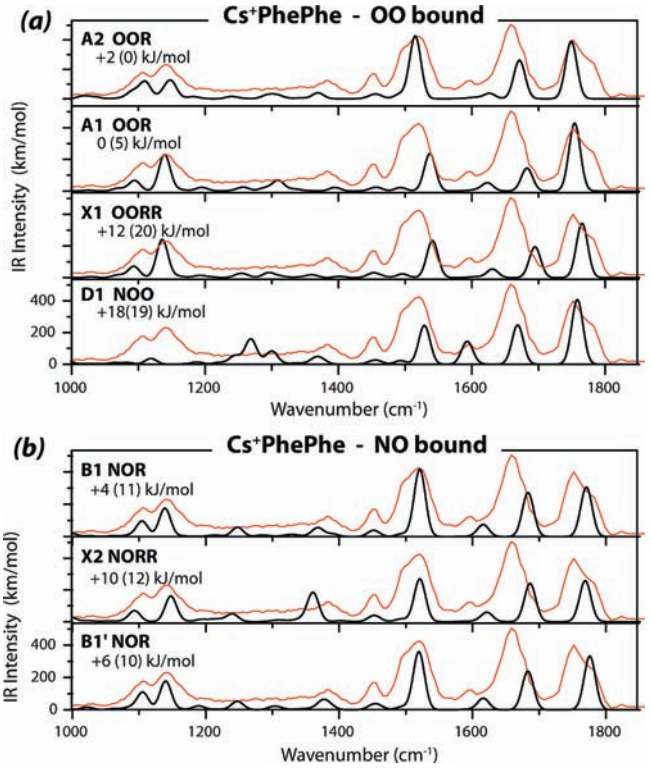

Figure 8. (a) Calculated spectra (black) of Cs^+ complexes chelated by (a) the carboxy carbonyl oxygen and (b) the amino nitrogen. The IRMPD experimental spectrum is overlaid in red. Energy values are 0 K enthalpies, with free energies given in parentheses (kJ/mol).

Table 2. Calculated Binding Energies of PhePhe and PheAla Complexes[a]

	Cs^+	K^+	Na^+	Li^+	Ba^{2+}	Ca^{2+}	Ag^+
PheAla	135	190	263	350	563	702	328
PhePhe							
open	127	183	256	344	566	707	320
closed	115	173	242	327	597	746	323

[a] Energy of attachment to the most stable conformation calculated for the neutral molecule in kJ mol^{-1}.

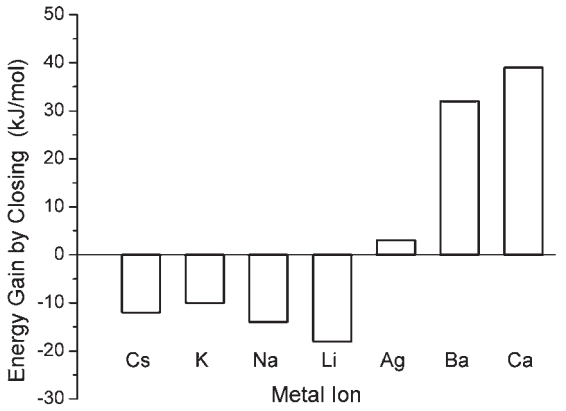

Figure 9. Computed energy gain for closing the "open" conformations. (difference in binding energy for the closed-cage conformation X1 and the open-cage conformation A1 (kJ mol^{-1}). Ions are ordered approximately according to overall binding energy (Table 2).

chelating position, and a closed-cage structure could be within the range of computational uncertainties). For K^+ and Cs^+ amino-bound complexes, the open-cage conformation B1 NOR appears to give the best spectroscopic match, but the closed-cage X2 conformation reproduces the experimental spectrum nearly as well and has approximately the same free energy. Thus, for the amino-bound fraction of the populations of these two heavier alkali-metal complexes, the open-cage NOR conformation is probably present, but contributions of other conformations, including closed cages, are quite possible. Note that for all alkali-metal ions, the spectra suggest that the carboxy-bound structures are substantially more abundant than the amino-bound structures, and we consider the former to be the ground states in all cases (as is also indicated by the calculated thermochemistry).

Finally, for Ag^+, only an amino-bound complex appears to be present, and uniquely among all the metal ions studied, it appears to have the closed-cage, amino-bound structure X2 NORR. Despite the apparent mismatch of relative intensities in the 1600–1700 cm^{-1} range, this structure gives the best overall agreement with the observed spectrum (see Figure S1 (Supporting Information)). Moreover, it is the most stable of all structures considered here. However, a contribution from the open-cage structure B1 NOR is not ruled out.

4. DISCUSSION

4.1. Binding and the Cation–π Interaction. The complexes of PheAla make a good reference comparison for evaluating the role of the two rings in PhePhe, since PheAla allows the same metal-ion binding interactions involving all of the Lewis basic sites (including the first ring), except that it lacks the possibility of a second cation–π interaction with the second ring in a "sandwich" or "closed cage" geometry. The computational results offer some insight into the strength of this latter interaction. Table 2 tracks the thermochemistry of the OOR conformations (the "open" geometry having only one cation–π interaction) of PhePhe and PheAla, as well as the OORR conformation (the "closed" geometry having cation–π interactions with both rings). Figure 9 displays graphically the trends of these binding energies.

The binding energies of PheAla and the "open" conformation of PhePhe are quite similar across the series, confirming that PheAla is a reasonable analogue. However, a clear contrast is seen between alkali-metal ions and alkaline-earth-metal ions with respect to the behavior of the "closed" conformation of PhePhe. For the singly charged alkali metals, closing the cage to go from the open conformation of PhePhe to the closed one is accompanied by an energy cost of about 10–20 kJ/mol, whereas for the doubly charged alkaline-earth-metal ions the closed conformation is *favored* by 30–40 kJ/mol. The strain energy that inhibits the complexes from folding into the closed conformation is not known, so we cannot make an exact calculation of the cation–π interaction energies, but we can conclude from this comparison that the cation–π interaction energy of the second ring, which tends to drive the geometry toward the closed form, is on the order of 50 kJ/mol larger for the doubly charged metal ions than for the singly charged ones. Graphically, Figure 9 shows clearly how the relative binding energy for the closed conformation jumps up sharply for the alkaline-earth-metal ions. The singly

dx.doi.org/10.1021/ja200219q | J. Am. Chem. Soc. 2011, 133, 9376–9386

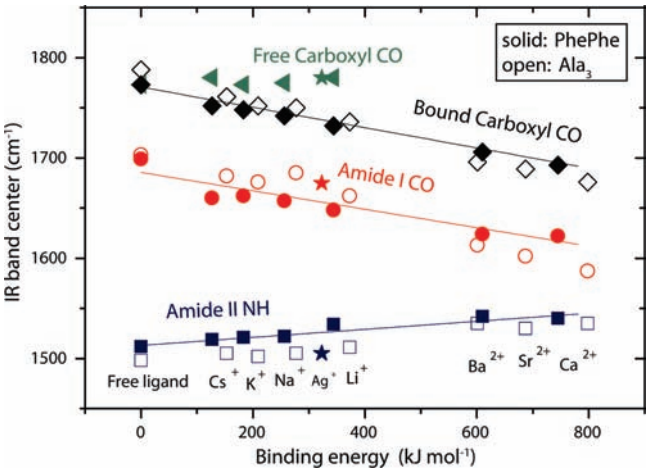

Figure 10. Shifts of the experimentally measured frequencies of selected vibrational modes plotted against the (computed) binding energies of the metal ions. (Frequencies of the uncomplexed neutral molecules, plotted at zero binding energy, are computed values.) Blue symbols show peaks assigned as amide II, red symbols as amide I, black symbols as the carboxyl CO stretching in a metal-bound configuration, and gray symbols as the unbound carboxyl CO stretching. Solid symbols are PhePhe complexes, and open symbols are complexes of AlaAlaAla.[39] Star symbols show the Ag^+ complex. Solid lines are linear fits to the PhePhe points (excluding Ag^+).

charged transition metal Ag^+ is intermediate, showing a greater willingness to form a second cation$-\pi$ interaction than the alkali metals, but much less than the doubly charged ions.

4.2. Vibrational Frequency Shifts. It has been interesting to follow the spectroscopic shifts of the IR-active normal modes in various classes of peptide complexes as a function of metal-ion identity.[31,39] The mode frequencies track the binding energies of the metal ions with reasonably accurate linearity, although the slopes and intercepts of the linear functions depend to some extent on the particular chelation environment of the metal ion in each type of complex. Surveying such trends for the PhePhe complexes, Figure 10 follows three prominent vibrational modes which show strong metal-induced frequency perturbations. These are the carboxyl C═O stretch, amide I (amide C═O plus C−N stretch), and amide II (amide N−H bend) bands. The frequencies of these modes in the complexes of AlaAlaAla (plotted as open symbols in Figure 10) were shown to shift linearly versus binding energy to the metal ion.[39] The corresponding PhePhe peak positions are plotted as closed symbols. Again, the linearity is good, with somewhat different slopes and intercepts. In particular, the slopes of the two carbonyl-dominated modes are distinctly lower for PhePhe than for Ala_3, which suggests that interaction with the carbonyl oxygens plays a smaller role in the overall chelation energy than was the case for Ala_3. This can be understood in terms of the additional solvation provided by the aromatic rings.

Note that all entries in Figure 10 are experimental (from Figure 4), except the points at "zero binding energy", which are computed values for conformations of the neutral molecule having intermolecular interactions similar to those in the metal-ion complexes. In principle the "open" alkali-metal complexes might not be expected to follow the same trends as the "closed" alkaline-earth-metal complexes, but as seen above (Figures 5−8), the frequencies of amide I and amide II vibrations differ little between open (OOR) and closed (OORR) chelation types; therefore, plotting all values in one graph is sensible. The appearance of a fraction of NOR structures in the alkali-metal complex spectra exposes a further set of distinct peaks for the "free" carboxyl C═O stretch. Since the relevant carbonyl oxygen is not chelated in this NOR conformation, the frequencies for these NOR complexes (plotted in green in Figure 10) are expected to differ little from the neutral molecule, and it is seen that they are indeed all close to the 1773 cm^{-1} frequency calculated for the free carboxyl stretch of noninteracting neutral PhePhe. Again, the calculations suggest that amide I and amide II frequencies are not very different between the OOR, OORR, and NOR conformations, so that plotting a single frequency point for each of these two modes for each metal ion, without needing to guess which structure dominates the spectrum in each case, is a reasonable approximation.

Values for the Ag^+PhePhe complex are also plotted in Figure 10, with star symbols. The assigned X2 conformation has no "bound carboxyl CO" mode; thus, it is correct to compare the carboxyl C═O stretching frequency with the "free carboxyl CO" stretching mode of the alkali-metal complexes. They are indeed seen to agree very well. The frequency shifts of the amide I and amide II modes for the Ag^+ complex do not follow the trend of the nearby alkali PhePhe complexes very well, being significantly smaller for both bands. The binding interactions, size of the ion, and other properties of Ag^+ are so different that we will not attempt to analyze the reasons for this divergence. The values for Ag^+ with PhePhe agree quite well with those for the Ag^+ complex of Ala_3, which is an observation that invites further investigation.

5. CONCLUSIONS

IRMPD spectroscopy and quantum-chemical computations have been applied to investigate the structures formed upon binding of singly and doubly charged ions to the PhePhe dipeptide ligand. The major point of interest in these results is the high stability of the caged complexes for the alkaline-earth-metal 2+ cations. A possible encapsulation motif involving double aromatic cation$-\pi$ interaction for highly charged metal ions in peptide environments is thus exposed that has not been previously considered. The closed-cage conformation is of the order of 30−40 kJ/mol more stable than the best open conformations (20−30 kJ/mol in free energy terms), showing that this encapsulation motif is highly favorable. In contrast, the singly charged alkali-metal complexes have a 10−20 kJ/mol preference to form an open-cage structure, giving complexes with only one of the aromatic rings bound to the metal ion. The indication that the cation$-\pi$ solvation interaction and metal-ion sequestration is much more effective for more highly charged metal ions could have implications in the understanding of such effects in nonpolar solvents or in the hydrophobic interior of solution-phase peptides.

Linear correlations of the strongly perturbed vibrational mode frequencies versus metal ion binding strength are shown here as a pointer toward future deeper analysis. A more incisive relation may be possible by correlating the perturbations of vibrational frequencies against localized metal−ligand interaction effects, e.g., through the examination of specific metal−ligand bond lengths, but this is not a simple relation to work out quantitatively. Rather than attempting correlations against bond lengths, it seems more useful to focus on an "intrinsic" metal−ligand

interaction energy, working from the overall binding energy and correcting for the distortion energy cost of deforming the original neutral ligand into the metal-complexed geometry. These distortion energies are calculated to be on the order of 65 kJ mol^{-1} for all the singly charged ions and 100 kJ mol^{-1} for the doubly charged systems. Correcting for such effects will result in modest changes in the slopes of correlation plots such as Figure 10 but will not affect the overall conclusion of approximate linearity of the correlations. Such considerations will be important in future efforts to quantify vibrational frequency perturbations, which can be illuminated by new spectroscopic methods such as those exploited here.

The unique preference of the Ag^+ complex for metal chelation by the amino nitrogen, combined with a closed-cage conformation, sets it apart from the behavior of the main-group-metal cations. Whether this reflects a special nitrogen affinity of Ag^+ or is a more general characteristic of transition-metal complexation of the dipeptide will have to be resolved by study of additional transition-metal-ion complexes.

■ ASSOCIATED CONTENT

Supporting Information. Text giving the complete ref 60 and figures giving IRMPD and calculated spectra of MPhePhe for $M = Ag^+$, Ca^{2+}, Na^+. This material is available free of charge via the Internet at http://pubs.acs.org.

■ AUTHOR INFORMATION

Corresponding Author

*E-mail: rcd@po.cwru.edu (R.C.D.); J.Oomens@rijnhuizen.nl (J.O.).

Present Addresses

[§]Sandia/California, 7011 East Avenue, Livermore, CA 94551-0969.

■ ACKNOWLEDGMENT

This work was financially supported by the "Nederlandse Organisatie voor Wetenschappelijk Onderzoek" (NWO). R.C.D. acknowledges support from the National Science Foundation, Grant PIRE-0730072, and expresses gratitude to the FOM for its continuing welcome. J.O. acknowledges support from the Stichting Physica. The FELIX staff, and particularly Dr. Lex van der Meer, Dr. Britta Redlich, and Dr. Giel Berden, are gratefully acknowledged for their assistance.

■ REFERENCES

(1) Enoki, T., Suzuki, M., Endo, M. *Graphite Intercalation Compounds and Applications*; Oxford University Press: London, 2003.
(2) van Heijnsbergen, D.; von Helden, G.; Meijer, G.; Maître, P.; Duncan, M. A. *J. Am. Chem. Soc.* **2002**, *124*, 1562–1563.
(3) Eyler, J. R. *Mass Spectrom. Rev.* **2009**, *28*, 448–467.
(4) Polfer, N. C.; Oomens, J. *Mass Spectrom. Rev.* **2009**, *28*, 468–494.
(5) Duncan, M. A. *Int. J. Mass Spectrom.* **2000**, *200*, 545–569.
(6) Duncan, M. A. *Int. J. Mass Spectrom.* **2008**, *272*, 99–118.
(7) Serra, G.; Chaudret, B.; Saillard, Y.; Lebeuze, A.; Rabaa, H.; Ristorcelli, I.; Klotz, A. *Astron. Astrophys.* **1992**, *260*, 489–493.
(8) Simon, A.; Joblin, C. *J. Phys. Chem. A* **2009**, *113*, 4878–4888.
(9) Reddy, A. S.; Sastry, G. M.; Sastry, G. N. *Proteins: Struct., Funct., Bioinf.* **2007**, *67*, 1179–1184.
(10) Gallivan, J. P.; Dougherty, D. A. *Proc. Natl. Acad. Sci. U.S.A.* **1999**, *96*, 9459.
(11) Ma, J. C.; Dougherty, D. A. *Chem. Rev.* **1997**, *97*, 1303–1324.
(12) Dougherty, D. A. *Science* **1996**, *271*, 163.
(13) Dougherty, D. A.; Lester, H. A. *Angew. Chem., Int. Ed.* **1998**, *37*, 2329.
(14) Mecozzi, S.; West, A. P. J.; Dougherty, D. A. *J. Am. Chem. Soc.* **1996**, *118*, 2307–2308.
(15) Zhong, W. G.; Gallivan, J. P.; Zhang, Y. N.; Li, L. T.; Lester, H. A.; Dougherty, D. A. *Proc. Natl. Acad. Sci. U.S.A.* **1998**, 95.
(16) DeWall, S. L.; Meadows, E. S.; Barbour, L. J.; Gokel, G. W. *J. Am. Chem. Soc.* **1999**, *121*, 5613.
(17) Hu, J.; Barbour, L. J.; Gokel, G. W. *Proc. Natl. Acad. Sci. U.S.A.* **2002**, *99*, 5121–5126.
(18) DeWall, S. L.; Meadows, E. S.; Barbour, L. J.; Gokel, G. W. *Proc. Natl. Acad. Sci. U.S.A.* **2000**, *97*, 6271–6276.
(19) Minoux, H.; Chipot, C. *J. Am. Chem. Soc.* **1999**, *121*, 10366.
(20) Hallowita, G. N. Ph.D. Thesis, Structural and thermochemical studies of cation-pi interactions; Wayne State University, ETD Collection for Wayne State University, 2010 Paper AAI1483807.
(21) Kish, M. M.; Ohanessian, G.; Wesdemiotis, C. *Int. J. Mass Spectrom.* **2003**, *227*, 509–524.
(22) Cabarcos, O. M.; Weinheimer, C. J.; Lisy, J. M. *J. Chem. Phys.* **1999**, *110*, 8429–8435.
(23) Hu, P.; Sorensen, C.; Gross, M. L. *J. Am. Soc. Mass Spectrom.* **1995**, *6*, 1079.
(24) Gokel, G. W.; Barbour, L. J.; De Wall, S. L.; Meadows, E. S. *Coord. Chem. Rev.* **2001**, *222*, 127–154.
(25) Gokel, G. W.; Barbour, L. J.; Ferdani, R.; Hu, J. *Acc. Chem. Res.* **2002**, *35*, 878–886.
(26) Bojesen, G.; Brendahl, T.; Anderson, U. *Org. Mass Spectrom.* **1993**, *28*, 1448.
(27) Shoeib, T.; Siu, K. W. M.; Hopkinson, A. C. *J. Phys. Chem. A* **2002**, *106*, 6121–6128.
(28) Ruan, C. H.; Rodgers, M. T. *J. Am. Chem. Soc.* **2004**, *126*, 14600–14610.
(29) Siu, F. M.; Ma, N. L.; Tsang, C. W. *Chem.—Eur. J.* **2004**, *10*, 1966–1976.
(30) Ryzhov, V.; Dunbar, R. C.; Cerda, B.; Wesdemiotis, C. *J. Am. Chem. Soc.* **2000**, *11*, 1037–1046.
(31) Dunbar, R. C.; Steill, J. D.; Oomens, J. *Phys. Chem. Chem. Phys.* **2010**, *12*, 1–11.
(32) Dunbar, R. C.; Steill, J. D.; Polfer, N. C.; Oomens, J. *J. Phys. Chem. A* **2009**, *113*, 845.
(33) Polfer, N. C.; Oomens, J.; Moore, D. T.; von Helden, G.; Meijer, G.; Dunbar, R. C. *J. Am. Chem. Soc.* **2006**, *128*, 517–525.
(34) Cerda, B. A.; Wesdemiotis, C. *J. Am. Chem. Soc.* **1995**, *117*, 9734.
(35) Lee, V. W.-M.; Li, H.; Lau, T.-C.; Guevremont, R.; Siu, K. W. M. *J. Am. Soc. Mass Spectrom.* **1998**, *9*, 760.
(36) Lucas, B.; Gregoire, G.; Lemaire, J.; Maître, P.; Ortega, J.-M.; Rupenyan, A.; Reimann, B.; Schermann, J. P.; Desfrançois, C. *Phys. Chem. Chem. Phys.* **2004**, *6*, 2659–2663.
(37) Polfer, N. C.; Oomens, J.; Dunbar, R. C. *ChemPhysChem* **2008**, *9*, 579–589.
(38) Klassen, J. S.; Anderson, S. G.; Blades, A. T.; Kebarle, P. *J. Phys. Chem.* **1996**, *100*, 14218–14227.
(39) Dunbar, R. C.; Steill, J. D.; Oomens, J. *Int. J. Mass Spectrom.* **2010**, *297*, 107–115.
(40) Dunbar, R. C.; Steill, J.; Polfer, N. C.; Oomens, J. *J. Phys. Chem. B* **2009**, *113*, 10552–10554.
(41) Stearns, J. A.; Guidi, M.; Boyarkin, O. V.; Rizzo, T. R. *J. Chem. Phys.* **2007**, *127*, 154322.
(42) Cerda, B. A.; Hoyau, S.; Ohanessian, G.; Wesdemiotis, C. *J. Am. Chem. Soc.* **1998**, *120*, 2437.
(43) Benzakour, M.; McHarfi, M.; Cartier, A.; Daoudi, A. *J. Mol. Struct. (THEOCHEM)* **2004**, *710*, 169–174.
(44) Prell, J. S.; Flick, T. G.; Oomens, J.; Berden, G.; Williams, E. R. *J. Phys. Chem. A* **2010**, *114*, 854–860.
(45) Wang, P.; Wesdemiotis, C.; Kapota, C.; Ohanessian, G. *J. Am. Soc. Mass Spectrom.* **2007**, *18*, 541–552.

(46) Oomens, J.; Polfer, N.; Moore, D. T.; van der Meer, L.; Marshall, A. G.; Eyler, J. R.; Meijer, G.; von Helden, G. *Phys. Chem. Chem. Phys.* **2005**, *7*, 1345–1348.
(47) Macias, A. T.; Norton, J. E.; Evanseck, J. D. *J. Am. Chem. Soc.* **2003**, *125*, 2351–2360.
(48) Santarelli, V. P.; Eastwood, A. L.; Dougherty, D. A.; Ahern, C. A.; Horn, R. *Biophys. J.* **2007**, *93*, 2341–2349.
(49) Carafoli, E. *FEBS J.* **2005**, *272*, 1073–1089.
(50) The UniProt Consortium, Ongoing and future developments at the Universal Protein Resource, Nucleic Acids Res. 39: D214-D219, 2011.
(51) Martinez Gil, A. C. M. A.; Medina Padilla, M., Munoz Ruiz, P.; Rubio Arrieta, L.; Garcia Palomero, E.; De Austria, C. European Patent Appl., Appl. No. EP 1798220 A1, 2007.
(52) Wolff, J. M.; Sheldrick, W. S. *J. Organomet. Chem.* **1997**, *531*, 141–149.
(53) Tetreault, S.; Ananthanarayanan, V. S. *J. Med. Chem.* **1993**, *36*, 1017–1023.
(54) Polfer, N. C.; Oomens, J.; Dunbar, R. C. *Phys. Chem. Chem. Phys.* **2006**, *8*, 2744–2751.
(55) Mino, W. K., Jr.; Szczepanski, J.; Pearson, W. L.; Powell, D. H.; Dunbar, R. C.; Eyler, J. R.; Polfer, N. C. *Int. J. Mass Spectrom.* **2010**, *297*, 131–138.
(56) Dunbar, R. C.; Polfer, N. C.; Oomens, J. *J. Am. Chem. Soc.* **2007**, *129*, 14562–14563.
(57) Moore, D. T.; Oomens, J.; Eyler, J. R.; von Helden, G.; Meijer, G.; Dunbar, R. C. *J. Am. Chem. Soc.* **2005**, *127*, 7243–7254.
(58) Dunbar, R. C.; Moore, D. T.; Oomens, J. *J. Phys. Chem. A* **2006**, *110*, 8316–8326.
(59) Simon, A.; Jones, W.; Ortega, J.-M.; Boissel, P.; Lemaire, J.; Maître, P. *J. Am. Chem. Soc.* **2004**, *126*, 11666–11674.
(60) Frisch, M. J.; et al. *Gaussian 03, Revision B.04*; Gaussian, Inc., Pittsburgh, PA, 2003.
(61) Weigend, F.; Ahlrichs, R. *Phys. Chem. Chem. Phys.* **2005**, *7*, 3297.
(62) Carl, D. R.; Cooper, T. E.; Oomens, J.; Steill, J. D.; Armentrout, P. B. *Phys. Chem. Chem. Phys.* **2010**, *12*, 3384–3398.
(63) Heaton, A. L. B. V. N.; Oomens, J.; Steill, J. D.; Armentrout, P. B. *J. Phys. Chem. A* **2009**, *113*, 5519–5530.
(64) Zhao, Y.; Truhlar, D. G. *Acc. Chem. Res.* **2008**, *41*, 157–167.
(65) Oh, H. B.; Lin, C.; Hwang, H. Y.; Zhai, H.; Breuker, K.; Zabrouskov, V.; Carpenter, B. K.; McLafferty, F. W. *J. Am. Chem. Soc.* **2005**, *127*, 4076–4083.
(66) Valle, J.; Eyler, J. R.; Oomens, J.; Moore, D. T.; van der Meer, A. F. G.; von Helden, G.; Meijer, G.; Hendrickson, C. L.; Marshall, A. G.; Blakney, G. T. *Rev. Sci. Instrum.* **2005**, *76*, 023103.
(67) Polfer, N. C.; Oomens, J. *Phys. Chem. Chem. Phys.* **2007**, *9*, 3804–3817.
(68) Drayss, M. K.; Armentrout, P. B.; Oomens, J.; Schaefer, M. *Int. J. Mass Spectrom.* **2010**, *297*, 18–27.
(69) Kapota, C.; Lemaire, J.; Maître, P.; Ohanessian, G. *J. Am. Chem. Soc.* **2004**, *126*, 1836–1842.
(70) Bush, M. F.; Forbes, M. W.; Jockusch, R. A.; Oomens, J.; Polfer, N. C.; Saykally, R. J.; Williams, E. R. *J. Phys. Chem. A* **2007**, *111*, 7753–7760.
(71) Bush, M. F.; O'Brien, J. T.; Prell, J. S.; Saykally, R. J.; Williams, E. R. *J. Am. Chem. Soc.* **2007**, *129*, 1612–1622.
(72) Bush, M. F.; Prell, J. S.; Saykally, R. J.; Williams, E. R. *J. Am. Chem. Soc.* **2007**, *129*, 13544–13553.
(73) Forbes, M. W.; Bush, M. F.; Polfer, N. C.; Oomens, J.; Dunbar, R. C.; Williams, E. R.; Jockusch, R. A. *J. Phys. Chem. A* **2007**, *111*, 11759–11770.
(74) Bush, M. F.; Oomens, J.; Williams, E. R. *J. Phys. Chem. A* **2009**, *113*, 431–438.
(75) Dunbar, R. C.; Hopkinson, A. C.; Oomens, J.; Siu, C.-K.; Siu, K. W. M.; Steill, J. D.; Verkerk, U. H.; Zhou, J. *J. Phys. Chem. B* **2009**, *113*, 10403–10408.
(76) Bush, M. F.; Oomens, J.; Saykally, R. J.; Williams, E. R. *J. Am. Chem. Soc.* **2008**, *130*, 6463–6471.
(77) O'Brien, J. T.; Prell, J. S.; Steill, J. D.; Oomens, J.; Williams, E. R. *J. Phys. Chem. A* **2008**, *112*, 10823–10830.
(78) Armentrout, P. B.; Rodgers, M. T.; Oomens, J.; Steill, J. D. *J. Phys. Chem. A* **2008**, *112*, 2248–2257.
(79) Rodgers, M. T.; Armentrout, P. B.; Oomens, J.; Steill, J. D. *J. Phys. Chem. A* **2008**, *112*, 2258–2267.
(80) Citir, M.; Stennett, E. M. S.; Oomens, J.; Steill, J. D.; Rodgers, M. T.; Armentrout, P. B. *Int. J. Mass Spectrom.* **2010**, *297*, 9–17.
(81) Fenn, L. S.; McLean, J. A.. *Anal. Bioanal. Chem.* **2008**, *391*, 905–909.